Optica Applicata, Vol. XLV, No. 1, 2015
DOI: 10.5277/oa150110

SO(3) matrix transformation for rapid polarization search and coding in a three-plate polarizer

CHUNHUI HUANG*, XUEJIN WANG

College of Physics and Information Engineering,
Fuzhou University, Fuzhou 350108, China

*Corresponding author: hchuang@fzu.edu.cn

A SO(3) transformer of a three-plate polarizer is adopted to rapidly achieve the transformation of the polarized state. The polarization coding based on Stokes components S_2 and S_3 is analyzed and demonstrated. Tabu search algorithm is used to accelerate the transformation of the polarized state by utilizing Mueller matrix roots decomposition to decompose the SO(3) matrix, and substituting first order Taylor series approximations for the trigonometric functions in the SO(3) matrix. The results show that bias voltage is less than 120 V in the coding zone. The search speed of our algorithm is faster than the one without first order Taylor series approximations by 4 times.

Keywords: SO(3) transformer, tabu search, polarization coding.

1. Introduction

Continuous variable quantum communication (CVQC) [1] is a promising scheme utilizing the quantum nature of light to guarantee the security in communication. There are two main types of CVQC: one is using squeezed states [2] or entangled states [3] and the other is using quantum coherent states [4]. Continuous variable coherent schemes are more attractive due to their high efficiency and compatibility [5]. They usually take the amplitude and phase of light as modulation parameters [6–11]. In our system, we use a new approach, a single-mode spatial signal transmission scheme [12], to simplify the setup of CVQC. The signal is a weak branch of polarized coherent light, and the local oscillator (LO) is a strong branch. One of the Stokes parameters S_2 and S_3 is randomly selected as a signal, and the other as a LO. Therefore, the single spatial beam including the signal and LO propagates in the free space, and the Stokes parameters are obtained by measuring the intensity of polarized lights [13].

In a single-mode spatial optical system, it is necessary to adopt a polarization controller with high speed and precision to efficiently carry information [14]. A SO(3) transformer based on $LiNbO_3$ crystal [15] has a high speed of polarization transformation,

so it is suitable to integrate as a polarization encoder. In this paper, we perform the transformation between two polarized states (PSs) based on a tabu search (TS) algorithm [16]. Considering that the electro-optic (EO) crystal can be equivalent to the plate capacitor, the bias voltage on it cannot be changed dramatically. Therefore, it is necessary to decompose the SO(3) matrix by dividing a large voltage into several small voltages with the Mueller matrix roots decomposition (MMRD) [17, 18] technique. Meanwhile, we apply the first order Taylor series approximations (FOTSA) [19] to replace the trigonometric function of the SO(3) matrix.

2. Polarization coding with SO(3) transformer

2.1. Design of SO(3) transformer

When polarized light passes through the EO-crystal, there is a phase retardance between the input polarized state (PS) and the output PS due to the effect of a refraction index ellipsoid [20], and it will cause the changes of the PS. The above principle can be defined as a SO(3) transformation of the PS. So different PSs can be generated by controlling the refraction index ellipsoid. We choose the SO(3) transformer based on $LiNbO_3$ crystals as a control device, as shown in Fig. 1.

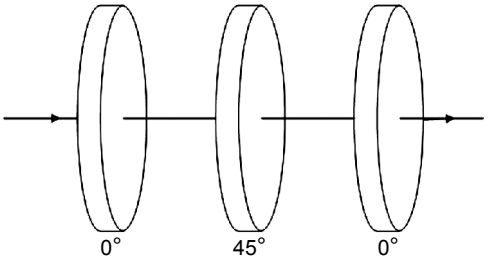

Fig. 1. The basic structure of SO(3) transformer.

The polarization transformation can be represented as a sub-matrix of Mueller's matrix, called the SO(3) matrix. To keep intuitional, we map the function of a SO(3) transformer in Fig. 1 to the Poincaré sphere. The first and third crystals make the PS rotate around the OS_1 axis on the sphere. The second crystal makes the PS rotate around the OS_2 axis. The radian represents the phase retardance introduced by $LiNbO_3$ crystal. The relationship between the phase retardance δ and the bias voltage V of the SO(3) transformer [13] is: $\delta = 0.006542V + 1.571$ at $\theta = 0°$ and $\delta = 0.0049V$ at $\theta = 45°$, where θ is the angle between the crystal axis and the horizontal direction. For a given angle θ, the relationship between the SO(3) matrix M and δ is as follows:

$$M(0°, \delta) = \begin{bmatrix} 1 & 0 & 0 \\ 0 & \cos\delta & \sin\delta \\ 0 & -\sin\delta & \cos\delta \end{bmatrix}, \quad M(45°, \delta) = \begin{bmatrix} \cos\delta & 0 & -\sin\delta \\ 0 & 1 & 0 \\ \sin\delta & 0 & \cos\delta \end{bmatrix} \tag{1}$$

The transformation of the PS is $M_{\mathrm{SO(3)}} = M_3(0°, \delta_3)M_2(45°, \delta_2)M_1(0°, \delta_1)$. So we can deduce the transformational relationship from Eq. (1): $[S_{\mathrm{out1}}, S_{\mathrm{out2}}, S_{\mathrm{out3}}]^T = M_{\mathrm{SO(3)}}[S_{\mathrm{in1}}, S_{\mathrm{in2}}, S_{\mathrm{in3}}]^T$, where $(M_{\mathrm{SO(3)}})_{11} = \cos\delta_2$, $(M_{\mathrm{SO(3)}})_{12} = \sin\delta_1\sin\delta_2$, $(M_{\mathrm{SO(3)}})_{13} = -\cos\delta_1\sin\delta_2$, …, $(M_{\mathrm{SO(3)}})_{33} = (\cos\delta_1\cos\delta_2\cos\delta_3 - \sin\delta_1\sin\delta_3)$. Therefore, we can use the transformational relationship to realize polarization coding by applying the corresponding bias voltages to the SO(3) transformer.

2.2. Polarization coding system

Considering the optical system in Fig. 2**a**, the encoder is a SO(3) transformer, and the decoder is a set of SO(3) + HWP. The encoding process is as follows: if an input is a random code a_m, it would be converted to a control signal $C_{A,\,m}$ and drives the control circuit to transform the input PS p_{in} to a new PS p_{o1}. Similarly, the decoding

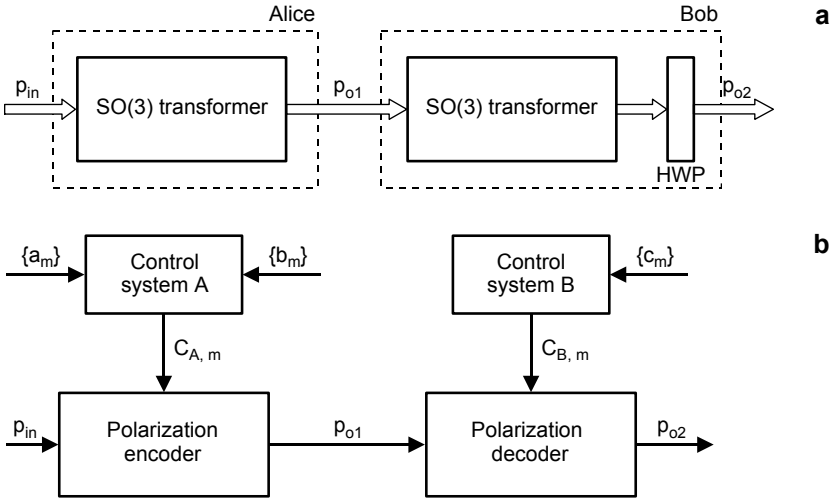

Fig. 2. Schematic of an optical system (**a**). Functional diagram of the optical system (**b**).

process is that the control system outputs a corresponding control signal $C_{B,\,m}$ acting on the decoder to transform p_{o1} to the output PS p_{o2}. The procedure of polarization coding is the following: let T_e be the transformation of a_m to $C_{A,\,m}$, represented as: $C_{A,\,m} = T_e\{a_m, b_m\}$, where b_m is the selection of the coding object; a_m follows Gaussian distribution for its maximum entropy of a mean value and variance among all known probability distributions [21]. We present the relationship between $C_{A,\,m}$ and the SO(3) matrix M_{PE} as $M_{\mathrm{PE}} = M\{C_{A,\,m}\}$. Then p_{in} would be transformed to p_{o1} as

$$p_{o1} = M_{\mathrm{PE}}\, p_{\mathrm{in}} \tag{2}$$

During the decoding process, let T_d represent the transformation of c_m to $C_{B,\,m} = T_d\{c_m\}$, where c_m is the randomly selection of measurement bases. We define the trans-

formation between $C_{B,m}$ and the SO(3) matrix M_{PD} as $M_{\mathrm{PD}} = M\{C_{B,m}\}$. For a given p_{in}, the output PS of our system is

$$p_{o2} = M_{\mathrm{PD}} M_{\mathrm{PE}} p_{\mathrm{in}} \tag{3}$$

2.3. Selection of measurement bases

For the security of CVQC, a single-mode light beam should meet the following three requirements:

1) The signal should be weak enough (about hundreds of photons) to ensure quantum natures [22].

2) The intensity of LO, which operates as an amplifier, should be much greater than the signal.

3) Components of the signal can be selected randomly as measurement bases to ensure that the communication process is in conformity with BB84 or B92 protocol [23].

In the single-mode spatial signal transmission scheme, considering that S_2 and S_3 are a pair of non-commutative components, Alice can select randomly one of S_2 and S_3 as a signal. Both the signal and the LO can then be transmitted in the same light path.

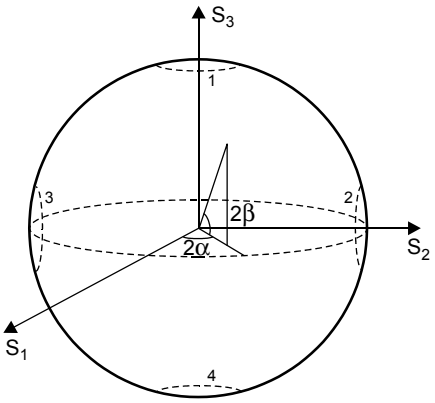

Fig. 3. Stokes parameters and the Poincaré sphere.

In terms of our transmission scheme, a threshold T (from 0.95 to 0.98) is set. If we choose S_3 as a signal, it requires $S_2 \geq T$; and if S_2 is the signal, it requires $S_3 \geq T$. It means that the polarization transformation is limited to two small zones of the Poincaré sphere. In Figure 3, S_2/S_3 is very small in the zone 1 or zone 4 while S_3 is much smaller than S_2 in the zone 2 or zone 3. Here we choose the zone 1 and zone 2 as coding zones.

3. TS algorithm with MMRD and FOTSA approximations

In this section, we present an algorithm to search the target PS rapidly and precisely with the small bias voltage. Since the definitions of Stokes parameters are: $S_1 = S_0\cos(2\beta)\cos(2\alpha)$, $S_2 = S_0\cos(2\beta)\sin(2\alpha)$ and $S_3 = S_0\sin(2\beta)$, as shown in Fig. 3,

for a given initial PS $[S_{\text{in1}}, S_{\text{in2}}, S_{\text{in3}}]^T$ and a given target Stokes parameter S_{out2} or S_{out3}, there are multiple search paths. Our algorithm uses the TS procedure to find the best search path. The tabu list [24] and neighborhood structure are two key roles in TS. The former has two main purposes: to prevent the return to the most recent visited solutions in order to avoid cycling; to drive the search towards regions of the solution space not yet explored and with high potential of containing good solutions. The latter determines the extent and quality of the solution space explored.

For any candidate solution $S_{\text{can}} = [S_{\text{can1}}, S_{\text{can2}}, S_{\text{can3}}]^T$ (T denotes transpose), the objective function $f(S_{\text{can},\,i})$, which is defined as follows:

$$f(S_{\text{can},\,i}) = \left| S_{\text{out},\,i} - S_{\text{can},\,i} \right|, \qquad i = 2, 3 \tag{4}$$

where the subscript i represents the i-th crystal. Considering that the EO-crystal can be equivalent to the plate capacitor, and the bias voltage on it cannot be changed dramatically, so the SO(3) matrix $N(\delta)$ (the first or third crystal) of polarization transformation should be divided into k infinitesimal slices. The decomposition is as follows:

$$N(\delta) = N(\Delta\delta_1)\ldots N(\Delta\delta_{k-1})N(\Delta\delta_k) \tag{5}$$

which is equivalent to dividing large voltage into several small voltages, and then they are applied to the crystal incrementally. Due to the difficulty in realizing the digitization of the trigonometric function, we substitute the FOTSA for the trigonometric function of the SO(3) matrix. If $\Delta\delta_i \ll 1$,

$$N_i(\Delta\delta_i) = \begin{bmatrix} 1 & 0 & 0 \\ 0 & \cos(\Delta\delta_i) & \sin(\Delta\delta_i) \\ 0 & -\sin(\Delta\delta_i) & \cos(\Delta\delta_i) \end{bmatrix} \approx \begin{bmatrix} 1 & 0 & 0 \\ 0 & 1 & \Delta\delta_i \\ 0 & -\Delta\delta_i & 1 \end{bmatrix}, \qquad i = 1, 3 \tag{6}$$

It shows a linear relation between the phase retardance $\Delta\delta$ and $N(\Delta\delta)$. The second crystal is in the similar method. As the recurrence process $N_i(\delta_{i,\,k+1}) = N_i(\delta_{i,\,k})N_i(\Delta\delta_{i,\,k+1})$, combining with Eqs. (5) and (6), we can derive the following linear relation:

$$N_i(\delta_{i,\,k+1}) \approx \begin{bmatrix} 1 & 0 & 0 \\ 0 & g_{i,\,k+1} & l_{i,\,k+1} \\ 0 & -l_{i,\,k+1} & g_{i,\,k+1} \end{bmatrix}, \qquad i = 1, 3 \tag{7}$$

The recursion formula can be written as

$$\begin{cases} g_{i,\,1} = 1 \\ l_{i,\,1} = \Delta\delta_{i,\,1} \end{cases}, \quad \begin{cases} g_{i,\,k+1} = g_{i,\,k} - \mu\Delta\delta_{i,\,k}\, l_{i,\,k} \\ l_{i,\,k+1} = l_{i,\,k} + \nu\Delta\delta_{i,\,k}\, g_{i,\,k} \end{cases}, \qquad k = 1, 2, 3, \ldots, K \tag{8}$$

where K is the iteration, μ and ν are fitting coefficients. The phase retardance of the current PS is denoted by $\delta_{i,k}$ in our algorithm, then its neighborhood is shown as:

$$\delta^n_{i,k+1} = \delta_{i,k} + \Delta\delta^n_{i,k} \tag{9}$$

where $n = 1, 2, \ldots, N$ (N – the number of neighborhoods). We obtain the neighborhood of the bias voltage from Eq. (9). The possible variation of the crystal bias is $+\Delta V_{ij}$, 0 V or $-\Delta V_{ij}$. Then, the number N of the current PS can be expressed as $C_3^1 C_3^1 C_3^1 - 1 = 26$,

$$V'_{ij} = V_{ij} + \Delta V_{ij}, \quad i = 1, 2, 3, \quad j = 1, 2, \ldots, 26 \tag{10}$$

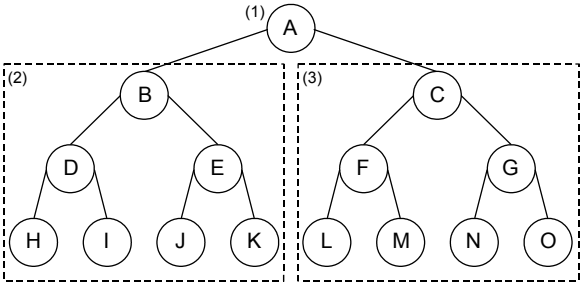

Fig. 4. Structure of the binary tree.

T a b l e 1. Pseudo-code of the tabu search algorithm.

```
Initialization
while f > 1×10^−3
    { /* Set neighborhood s_t */
    if f > 0.8 | S_b < 0.9, s_t = 0.5 /* S_b = S_2 or S_3
    elseif 0.5 ≤ f ≤ 0.8 | 0.9 ≤ S_b < 0.95, s_t = 0.2.
        else s_t = 0.1.
    Temp = Fitness(O_A); /* O_A denotes node A */
    while t_sign == 0
        { O_R → Child; /* O_R ∈ {O_B, O_C, …, O_O} */
        Calculate the solution of Child in the corresponding neighborhood;
        if Fitness(Child) < Temp
            { Temp = Fitness(Child);
            t_sign = 1;
            Save the corresponding solution; } }
    Let the optimal f* = Temp. /* Compare f* with f_1 in the tabu list */
    if f* < f_1
    { Reset tabu list and substitute current solution for the first solution in the Solution_list.
    Reorder f_i in tabu list in descending order. }
    Take current solution (V_out1, V_out2, V_out3) as initial solution (V_in1, V_in2, V_in3) in the next search process.
    if |V_in1| ≥ 150 | or |V_in2| ≥ 150 or |V_in3| ≥ 150
    { Reset parameters of SO(3) matrix g_1, l_1, g_2, l_2, g_3, l_3. }
    Increase counter Iteration. }
```

We use the binary tree structure to search the optimal neighborhood. The binary tree traversal is first from the top down, then from left to right [25, 26], as shown in Fig. 4. The 26 elements of neighborhood sets fall into 14 children and are stored in the respective node, where the corresponding PS of the node *A* is not changed. The result of this preorder traversal is *A-B-D-H-I-E-J-K-C-F-L-M-G-N-O*. According to the priority, we arrange the 14 children as: $+\Delta V_{ij} \rightarrow 0\ \text{V} \rightarrow -\Delta V_{ij}$. For example, the neighborhood sets $[+\Delta V_{ij}, +\Delta V_{ij}, +\Delta V_{ij}]$ and $[-\Delta V_{ij}, -\Delta V_{ij}, -\Delta V_{ij}]$ are in the node *B* and node *O*, respectively.

In the current neighborhood, according to Eq. (3), the PS is searched successively for each node of the binary tree until the value of the objective function f^* is no longer improved. The result at this time can be used as the candidate solution. Then f^* is compared with the maximum value f_1 in the tabu list. If f^* is smaller, f_1 is replaced by f^* and the values in the tabu list are reordered in a descending order. The depth of the tabu list is 16. The iteration is repeated until the optimal value is below 10^{-3}.

To satisfy the speed and accuracy requirement, we adopt the variable step-size. The search process includes three parts: if $f(S_{\text{can},\,i}) > 0.8$ or $S_b < 0.9$ (if $i = 2$, $S_b = S_3$), the search step is 0.5 V; if $0.5 \le f(S_{\text{can},\,i}) \le 0.8$ or $0.9 \le S_b < 0.95$, it is 0.2 V; if $f(S_{\text{can}}) < 0.5$, it is 0.1 V. The pseudo code of the above algorithm is shown in Table 1.

4. Simulation and coding verification

4.1. Performance of TS algorithm

To investigate the FOTSA, the simulation is carried out through 10^7 iterations on "Calculate the solution of *Child* in the corresponding neighborhood" in Table 1. Since it consumes most of time, we hope to reduce the run time by FOTSA. The results

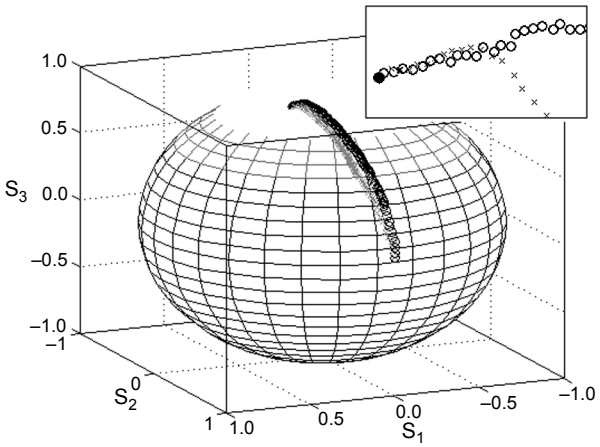

Fig. 5. The search path of polarization transformation; ○ – algorithm with FOTSA, and × – algorithm without FOTSA.

show that the speed of our algorithm is 4 times faster than the one without FOTSA. The former takes 0.17213 s and the latter is 0.911603 s (ratio 1/4).

The search path from the input PS $[0\ -1\ 0]^T$ to the target Stokes parameter $S_{out2} = 0.187$ at $S_{out3} \geq 0.95$ is simulated. The optimal search path is shown in Fig. 5. Each dot on the Poincaré sphere represents the current solution of the k-iteration during the search process. Considering the birefringence in the first and third crystals, the initial PS can be approximated to $[0\ 1\ 0]^T$. In the search process, PS changes continuously with the variation in the bias voltage. After a polarization transformation, the current solution is a new initial solution in the next transformation. Finally, if $f(S_{can,\,i})$ is less than 10^{-3}, we think that the current solution is agreed with the target PS (real dot). The deviation between the former and the target PS is larger than the latter. By simulation and optimization repeatedly, under the same condition, the final $f(S_{can,\,i})$ of the former is higher than the latter about two orders of magnitude.

In order to verify the feasibility of the algorithm, the 50 random PSs are simulated. The solid line in Fig. 6**a** is the distribution curve of Stokes parameters. The result shows that search values are agreed well with target values. Figure 6**b** shows the bias changes in the three crystals. When V_1 and V_3 range from –120 to 0 V, and V_2 ranges from –50

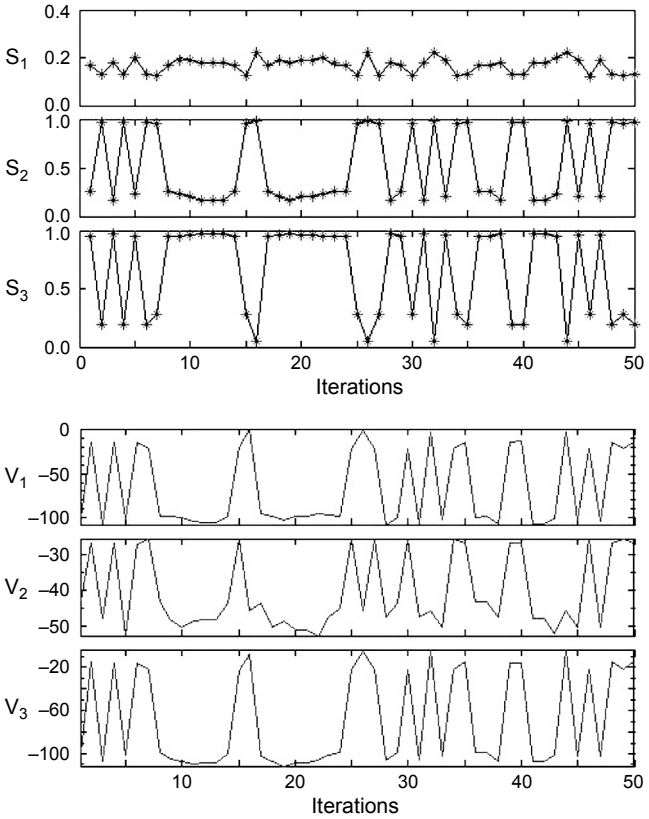

Fig. 6. The change of Stokes parameters (**a**) and the applied voltage on the crystal (**b**). * – search values.

to 0 V, all the PSs ($S_3 \geq 0.95$ or $S_2 \geq 0.95$) can be generated and the encoding of S_2 or S_3 can be implemented. HAO has built a polarization generator system based on a PZT squeezed fiber polarization controller, and its driving voltage is about 200 V [27]. However, the polarization generator of Hao's system is not an integrated device. On the contrary, SO(3) transformer is an integrated device, which is suitable for polarization coding in the free-space coherent optical communication. It must be emphasized that the maximum voltage of our control circuit is 150 V. Therefore, the requirement of our power supply circuit is lowered.

4.2. Coding verification

Octal random coding is simulated for verifying the function of the Stokes polarization coding. The input PS is $P_{\text{in}} = [0, -1, 0]^T$. Let $\{a_m\} = \{0, ..., 7\}$, $\{b_m\} = \{0, 1\}$, which represents S_3 or S_2 selected as a signal. For example, assuming the LO is $S_2 \geq 0.95$, the Gaussian random code $\{a_m\}$ is generated with the Box-Muller method [28]. We take a transformation T_e to obtain $C_{A,m} = \{V_1, V_2, V_3\}$. As described in Section 2.2, $C_{A,m}$ corresponds to the intervals $\{I_i\}$. To ensure that the LO is much greater than the signal, the coding signal is set within $[\beta_l, \beta_\mu]$, if Δ is the mean deviation between the search results and the expected values. To eliminate the code obfuscation caused by Δ, we partition coding zones as $I_1 = [\beta_l, \beta_l + D]$, $I_2 = [\beta_l + D + \Delta, \beta_l + 2D + \Delta]$, $I_3 = [\beta_l + 2D + 2\Delta, \beta_l + 3D + 2\Delta]$, …, and $I_8 = [\beta_\mu - D, \beta_\mu]$. Here, $\beta_l = 0.045$, $\beta_\mu = 0.195$, $D = 0.01$, $\Delta = 0.01$, as shown in Table 2. According to Eq. (2), p_{o1} is obtained, as shown in Fig. 7. The values of S_2 are in the top half of Fig. 7, and the cor-

T a b l e 2. Zones of code values.

Code	0	1	2	3	4	5	6	7
Values of S_3 [$\times 10^{-3}$]	45–55	65–75	85–95	105–115	125–135	145–155	165–175	185–195

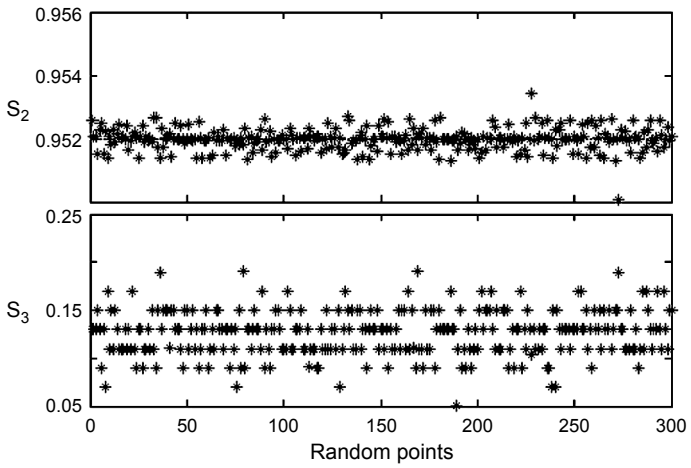

Fig. 7. Output of octal random encoding.

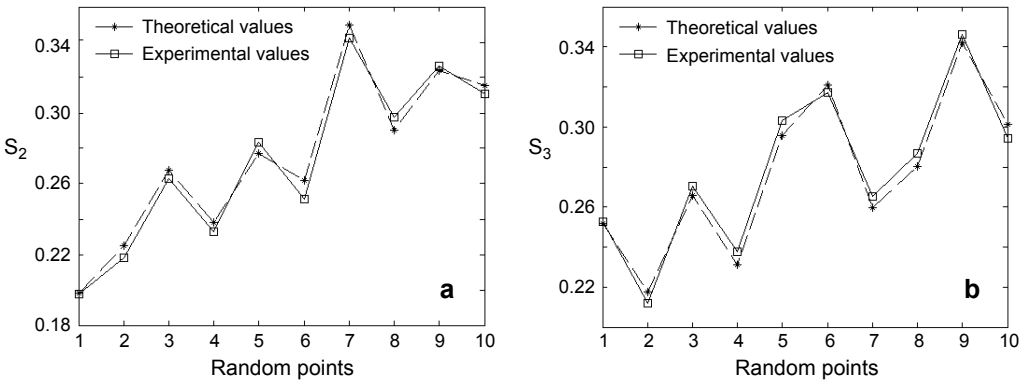

Fig. 8. The comparison of the experimental values and the theoretical values of S_2 (**a**) and S_3 (**b**).

responding code values of S_3 are in the bottom half; S_2 oscillates near 0.952, but it does not affect the final result; S_3 is agreed well with the corresponding range of $\{I_i\}$, and the codes can distinguish each other.

We compare the experimental values with the theoretical values of S_2 and S_3, respectively, as shown in Fig. 8. The result shows that the deviation is less than 0.01, therefore, $\Delta = 0.01$ is reasonable.

5. Conclusions

In this paper, we studied polarization search and the principle of coding by a SO(3) transformer. The transformer can be applied for both quantum and classical optical communication schemes, which depends on the characteristics of the signal. The two small zones on the Poincaré sphere were selected as coding zones. The Stokes parameters S_2 and S_3 were suitable as not only a pair of a signal and LO but also as a pair of measurement bases in the single-mode spatial signal transmission system. TS algorithm was applied to control the polarization coding. Also, MMRD and FOTSA were used to decompose the SO(3) matrix and replace the trigonometric function of the matrix, respectively. Moreover, octal random coding of the Stokes parameters was simulated. Results showed that the Stokes parameters were suitable for multilevel polarization coding, and the bias voltage was less than 120 V, which lowered the requirement of a power supply circuit.

Acknowledgements – This work is supported by the National Natural Science Foundation of China (Grant No. 61177072).

References

[1] SILBERHORN C., RALPH T.C., LÜTKENHAUS N., LEUCHS G., *Continuous variable quantum cryptography: beating the 3 dB loss limit*, Physical Review Letters **89**(16), 2002, article 167901.

[2] GARCÍA-PATRÓN R., CERF N.J., *Continuous-variable quantum key distribution protocols over noisy channels*, Physical Review Letters **102**(13) 2009, article 130501.

[3] XIAOLONG SU, AIHONG TAN, XIAOJUN JIA, JING ZHANG, CHANGDE XIE, KUNCHI PENG, *Experimental preparation of quadripartite cluster and Greenberger–Horne–Zeilinger entangled states for continuous variables*, Physical Review Letters **98**(7), 2007, article 070502.

[4] JOUGUET P., KUNZ-JACQUES S., LEVERRIER A., *Long-distance continuous-variable quantum key distribution with a Gaussian modulation*, Physical Review A **84**(6), 2011, article 062317.

[5] TAKESUE H., SAE WOO NAM, QIANG ZHANG, HADFIELD R.H., HONJO T., TAMAKI K., YAMAMOTO Y., *Quantum key distribution over a 40-dB channel loss using superconducting single-photon detectors*, Nature Photonics **1**(6), 2007, pp. 343–348.

[6] ZHIXIN LU, LI YU, KANG LI, BINGCAN LIU, JIANGUI LIN, RONGZHEN JIAO, BOJUN YANG, *Reverse reconciliation for continuous variable quantum key distribution*, Science China – Physics, Mechanics and Astronomy **53**(1), 2010, pp. 100–105.

[7] JOUGUET P., KUNZ-JACQUES S., DEBUISSCHERT T., FOSSIER S., DIAMANTI E., ALLÉAUME R., TUALLE-BROURI R., GRANGIER P., LEVERRIER A., PACHE P., PAINCHAULT P., *Field test of classical symmetric encryption with continuous variables quantum key distribution*, Optics Express **20**(13), 2012, pp. 14030–14041.

[8] JOUGUET P., KUNZ-JACQUES S., LEVERRIER A., GRANGIER P., DIAMANTI E., *Experimental demonstration of long-distance continuous-variable quantum key distribution*, Nature Photonics **7**(5), 2013, pp. 378–381.

[9] FURRER F., FRANZ T., BERTA M., LEVERRIER A., SCHOLZ V.B., TOMAMICHEL M., WERNER R.F., *Continuous variable quantum key distribution: Finite-key analysis of composable security against coherent attacks*, Physical Review Letters **109**(10), 2012, article 100502.

[10] WEEDBROOK C., LANCE A.M., BOWEN W.P., SYMUL T., RALPH T.C., PING KOY LAM, *Coherent--state quantum key distribution without random basis switching*, Physical Review A **73**(2), 2006, article 022316.

[11] LEVERRIER A., GRANGIER P., *Continuous-variable quantum-key-distribution protocols with a non-Gaussian modulation*, Physical Review A **83**(4), 2011, article 042312.

[12] ELSER D., BARTLEY T., HEIM B., WITTMANN C., SYCH D., LEUCHS G., *Feasibility of free space quantum key distribution with coherent polarization states*, New Journal of Physics **11**(4), 2009, article 045014.

[13] HUANG C., RONG W., *A control scheme of polarization generator based on three $LiNbO_3$ wave plates*, Laser & Optoelectronics Progress **50**(5), 2013, pp. 190–196.

[14] LI SHEN, MA HAI-QIANG, WU LING-AN, ZHAI GUANG-JIE, *High-speed polarization controller for all-fiber quantum communication systems*, Acta Physica Sinica **62**(8), 2013, article 084214.

[15] KOCH B., HIDAYAT A., HONGBIN ZHANG, MIRVODA V., LICHTINGER M., SANDEL D., NOÉ R., *Optical endless polarization stabilization at 9 krad/s with FPGA-based controller*, IEEE Photonics Technology Letters **20**(12), 2008, pp. 961–963.

[16] GLOVER F., ZHIPENG LÜ, JIN-KAO HAO, *Diversification-driven tabu search for unconstrained binary quadratic problems*, 4OR – A Quarterly Journal of Operations Research **8**(3), 2010, pp. 239–253.

[17] NOBLE H.D., CHIPMAN R.A., *Mueller matrix roots algorithm and computational considerations*, Optics Express **20**(1), 2012, pp. 17–31.

[18] DEVLAMINCK V., *Mueller matrix interpolation in polarization optics*, Journal of the Optical Society of America A **27**(7), 2010, pp. 1529–1534.

[19] FENG HUO, XUE-CHENG XI, AUN-NEOW POO, *Generalized Taylor series expansion for free-form two-dimensional contour error compensation*, International Journal of Machine Tools and Manufacture **53**(1), 2012, pp. 91–99.

[20] YAN-QING LU, ZHI-LIANG WAN, QUAN WANG, YUAN-XIN XI, NAI-BEN MING, *Electro-optic effect of periodically poled optical superlattice $LiNbO_3$ and its applications*, Applied Physics Letters **77**(23), 2000, pp. 3719–3721.

[21] HE YUN-XIAN, LU YUAN, ZHU JUN, PENG JIN-YE, ZENG GUI-HUA, *Gaussian-modulation in continuous--variable quantum communication*, Acta Sinica Quantum Optica **15**(4), 2009, pp. 329–335.

[22] GROSSHANS F., VAN ASSCHE G., WENGER J., BROURI R., CERF N.J., GRANGIER P., *Quantum key distribution using gaussian-modulated coherent states*, Nature **421**(6920), 2003, pp. 238–241.

[23] ETENGU R., ABBOU F.M., WONG H.Y., ABID A., NORTIZA N., SETHARAMAN A., *Performance comparison of BB84 and B92 satellite-based free space quantum optical communication systems in the presence of channel effects*, Journal of Optical Communications **32**(1), 2011, pp. 37–47.

[24] PAQUETTE J., CORDEAU J.-F., LAPORTE G., PASCOAL M.M.B., *Combining multicriteria analysis and tabu search for dial-a-ride problems*, Transportation Research Part B: Methodological **52**, 2013, pp. 1–16.

[25] BENTLEY J.L., *Multidimensional binary search trees used for associative searching*, Communications of the ACM **18**(9), 1975, pp. 509–517.

[26] CRAIN T., GRAMOLI V., RAYNAL M., *A speculation-friendly binary search tree*, ACM SIGPLAN Notices **47**(8), 2012, pp. 161–170.

[27] HAO JIAN, *Polarization generator research based on PZT squeezed fiber polarization controller*, Master's Thesis, Beijing Jiaotong University, 2011.

[28] LEE D.U., VILLASENOR J.D., LUK W., LEONG P.H.W., *A hardware Gaussian noise generator using the Box-Muller method and its error analysis*, IEEE Transactions on Computers **55**(6), 2006, pp. 659–671.

Received September 24, 2014